

## Regional structural differences across functionally parcellated Brodmann areas of human primary somatosensory cortex

Rosa Sanchez Panchuelo<sup>1</sup>, Julien Besle<sup>2</sup>, Olivier Mougin<sup>1</sup>, Penny Gowland<sup>1</sup>, Richard Bowtell<sup>1</sup>, Denis Schluppeck<sup>2</sup>, and Susan Francis<sup>1</sup>

<sup>1</sup>Sir Peter Mansfield Magnetic Resonance Centre, University of Nottingham, Nottingham, United Kingdom, <sup>2</sup>School of Psychology, University of Nottingham, Nottingham, United Kingdom

**Introduction:** Ultra-high-field (UHF) MRI is ideally suited to structural and functional imaging of the brain. Recent UHF MR studies have shown excellent *in-vivo* visualization of myelin content within gray matter (1) and good correspondence between functional (retinotopic) and structural (linked to myelination) parcellations of the primary visual cortex (V1) (2). In primary somatosensory cortex (S1), the base-to-tip mapping of the receptor sheet in the finger is reversed at the boundaries between areas 3a, 3b, 1, and 2 (3), providing a criterion allowing functional identification of Brodmann areas. Here, we use a travelling wave paradigm involving vibrotactile stimulation across the three phalanges of digits 2, 3 and 4 to identify the functional boundaries of areas 3b, 3a, 1 and 2, and investigate cortical thickness and myelin content variations across the underlying anatomy in these areas using high resolution structural MR data acquired *in-vivo*.

**Methods:** Four subjects participated in both functional and structural scanning sessions at 7 T. Functional areas were identified using a 'travelling wave' paradigm to produce mirror maps of the base-to-tip surface of digits 2, 3 and 4 of the left hand in S1 (4). Vibrotactile stimulation (30 Hz) was delivered to the skin using 9 independently controlled piezo-electric devices which each stimulated a ~1 mm<sup>2</sup> skin area (Figure 1A). The three phalanges of the three digits were each sequentially stimulated from base-to-tip for 8 s of a 24 s cycle, with 8 cycles being collected per run. GE-EPI (TR 2 s, TE 25 ms) was used to acquire 26 axial slices at 1.25 mm isotropic resolution. fMRI data were analysed using Fourier analysis and somatotopic (phase) maps were transformed onto flattened representations of the cortex to delineate functional ROIs based on the mirror maps of the finger representations. High resolution (0.5 mm isotropic resolution) Magnetization Transfer Ratio (MTR) data were acquired using a turbo field echo read-out and train of saturation pulses (5). T<sub>1</sub>-weighted Phase Sensitive Inversion Recovery (PSIR) data (0.3x0.3x1 mm<sup>3</sup> resolution) were also acquired using a sequence with two turbo field echo trains acquired at inversion delays of 785 (~ GM/WM null point) and 2685 ms after a single inversion pulse. The functionally defined ROIs were used to investigate anatomical differences in cortical thickness and myelin content reflected in the MTR and PSIR contrast. Quantification was performed in 2D folded space, based on the surfaces obtained from FreeSurfer. Cortical thickness was computed for each surface vertex, as the shortest distance between the white matter and pial surfaces, and since cortical thickness was highly correlated with the local surface curvature, curvature was regressed out from the thickness measure. Myelin content was estimated at each vertex by averaging MTR (or PSIR) data across the cortical depth.

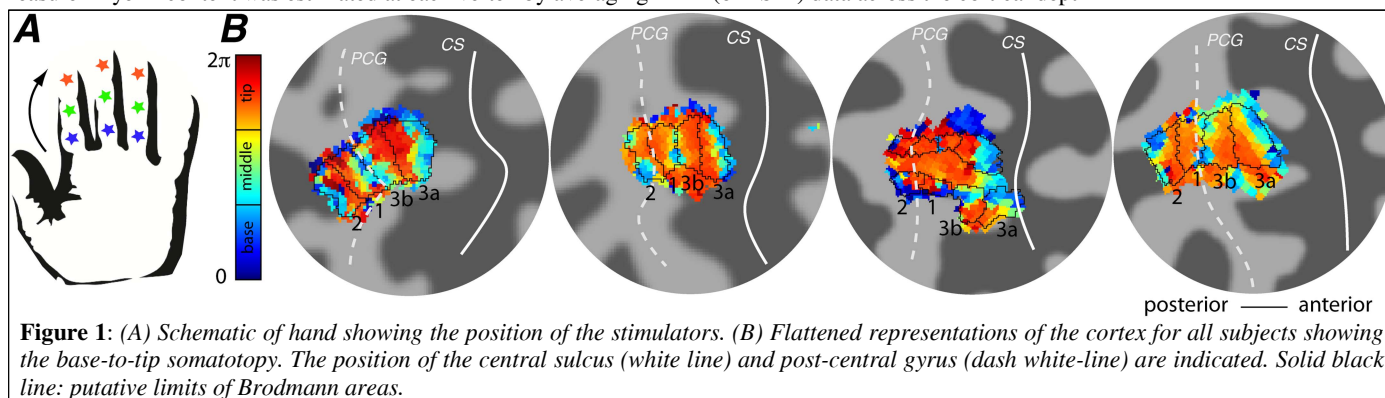


**Figure 1:** (A) Schematic of hand showing the position of the stimulators. (B) Flattened representations of the cortex for all subjects showing the base-to-tip somatotopy. The position of the central sulcus (white line) and post-central gyrus (dash white-line) are indicated. Solid black line: putative limits of Brodmann areas.

**Results:** Within-digit somatotopic maps (Figure 1B) show an orderly pattern of phase variation consistent with mirror representations in adjacent areas. Phase values alternate between orange (tip) and blue (base), with one reversal around the representation of the base and two reversals around the tip representation, suggesting the existence of four within-finger mirror maps (delineated by the solid black line). Quantitative comparisons of cortical thickness and myelin sensitive MR-measures showed regional differences across the different functional areas in S1 (Figure 2). The cortical thickness decreases on moving from anterior (area 2) to posterior (area 3a) and the mean MTR and PSIR measures across subjects suggest that area 3a is the less heavily myelinated area, with area 1 slightly more myelinated than areas 3b and 2.

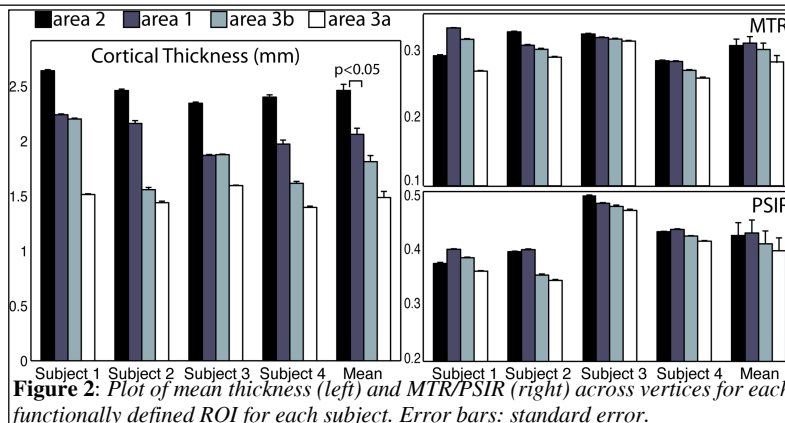


**Figure 2:** Plot of mean thickness (left) and MTR/PSIR (right) across vertices for each functionally defined ROI for each subject. Error bars: standard error.

**Discussion:** We have demonstrated within-digit functional parcellation of putative areas 3a, 3b, 1 and 2 of human primary somatosensory cortex based on mirror maps of the base-to-tip functional representation of the index, middle and ring finger. Regional differences in cortical thickness and myelin density were found across the functionally defined areas. Our measures of thickness are consistent with previous reports that gyral regions of the cortex are thicker than sulcal regions (6) with thickness of  $1.5 \pm 0.1$  and  $1.8 \pm 0.3$  mm measured in sulcal areas 3a and 3b respectively, comparable to previous results for cortical thickness in the posterior bank of the central sulcus ( $1.7 \pm 0.2$  mm (7)). The group MTR/PSIR data suggests that area 3a is less heavily myelinated than area 3b, and that area 2 has less myelin than area 1. This is at odds with light-field photomicrographs of myelin staining flattened cortex of macaque (8), which have revealed that area 3b is heavily myelinated, areas 3a and 2 are lightly myelinated and area 1 is moderately myelinated. However, for the measures used here structural differences were not significant between the sub-regions of S1. We conclude that at present functional mapping is a better tool for delineating sub-regions within S1.

**References:** (1) Geyer et al, *Front Hum Neurosci*, 5, 19, 2011. (2) Sanchez-Panchuelo et al, *JMRI*, 35:287-89, 2012. (3) Darian-Smith, *Ann Rev Psych* 33:155-94, 1982. (4) Sanchez-Panchuelo et al, *J Neurosci*, in press (5) Mougin et al., *NeuroImage*, 49:272-281, 2010. (6) Fischl & Dale, *PNAS*, 97:11050-55, 2002. (7) Meyer et al. *AJNR*, 17:1699-706, 1996. (8) Disbrow et al. *J Comp Neurol*, 462:382-99, 2003.